Magnetic Characteristics of New Cyano-Bridged Two-Dimensional Honeycomb-Like Bimetallic Assemblies Containing Ni(II)−N≡C−Cr(III) or Ni(II)−N≡C−Cr(I) Linkages

Hui-Zhong Kou, Song Gao,* Ou Bai, and Zhe-Ming Wang

State Key Laboratory of Rare Earth Materials Chemistry and Applications, College of Chemistry and Molecular Engineering, Peking University, Beijing 100871, P. R. China

Received March 14, 2001

Three cyano-bridged bimetallic assemblies, $[NiL^1]_3[Cr(CN)_6]_2\cdot 7H_2O$ (**1**), $[NiL^2]_3[Cr(CN)_6]_2\cdot 9H_2O$ (**2**), and $[NiL^2]_3[Cr(CN)_5(NO)]_2\cdot 9H_2O$ (**3**) (L^1 = 3,10-dimethyl-1,3,5,8,10,12-hexaazacyclooctadecane and L^2 = 3,10-diethyl-1,3,5,8,10,12-hexaazacyclooctadecane), have been prepared and characterized structurally and magnetically. Complex **1** crystallizes in the monoclinic space group of $C2/c$ with $a = 25.929$ Å, $b = 15.442(3)$ Å, $c = 19.553(4)$ Å, $\beta = 106.21(3)°$, and $Z = 4$, while **2** and **3** are in the trigonal space group $P\bar{3}$ with $a = b = 14.919(2)$ Å, $c = 9.5246(19)$ Å, $\gamma = 120°$, and $Z = 1$ for **2** and $a = b = 14.863(2)$ Å, $c = 9.3134(19)$ Å, $\gamma = 120°$, and $Z = 1$ for **3**. The structures of **1**−**3** are similar and consist of cyano-bridged two-dimensional (2D) honeycomb-like neutral Ni_3Cr_2 layers. In each complex, $[Cr(CN)_6]^{3-}$ or $[Cr(CN)_5(NO)]^{3-}$ coordinates to three *trans*-[Ni(macrocycle)]$^{2+}$ groups using three *fac*-CN^- ligands, providing a 2D layered network. The NO group in $[Cr(CN)_5(NO)]^{3-}$ remains monodentate. Magnetic studies show the existence of a short-range ferromagnetic interaction in all of the complexes. Complexes **1** and **2** exhibit long-range antiferromagnetic ordering at 13.0 and 11.9 K, respectively, and a metamagnetic transition with critical field of ca. 1.6 kOe for **1** and 1.5 kOe for **2** at 1.8 K. Complex **3** exhibits long-range ferromagnetic ordering below 4.3 K.

Introduction

There has been continuing interest in the magnetic chemistry of the cyano-bridged Prussian blue (PB) analogues of general composition $M_x[M'(CN)_6]_y\cdot nH_2O$.[1−14] This may be caused by the findings that some transition-metal cyanides exhibit long-range magnetic ordering above room temperature.[13] Recently, the studies on three-dimensional (3D) PB analogues derived from $M(CN)_8^{3-}$ or $Mo(CN)_7^{4-}$ building blocks emerged and received great attention.[15,16]

PB analogues of different dimensionalities have been extensively investigated with the aim of understanding the structure−property relationship.[17−39] Until now, zero-, one-, two-, and three-dimensional topologies have been reported and interesting

(1) Dunbar, K. R.; Heintz, R. A. *Prog. Inorg. Chem*. **1997**, *45*, 283 and references therein.
(2) Klenze, R.; Kanellakopulos, B.; Trageser, G.; Eysel, H. H. *J. Chem. Phys*. **1980**, *72*, 5819.
(3) Herren, F.; Fischer, P.; Ludi, A.; Hälg, W. *Inorg. Chem*. **1980**, *19*, 956.
(4) Griebler, W. D.; Babel, D. *Z. Naturforsch., B: Chem. Sci.* **1982**, *87*, 832.
(5) Gadet, V.; Mallah, T.; Castro, I.; Verdaguer, M. *J. Am. Chem. Soc*. **1992**, *114*, 9213.
(6) Mallah, T.; Thiebaut, S.; Verdaguer, M.; Veillet, P. *Science* **1993**, *262*, 1554.
(7) Entley, W. R.; Girolami, G. S. *Inorg. Chem*. **1994**, *33*, 5165.
(8) Entley, W. R.; Girolami, G. S. *Science* **1995**, *21*, 268.
(9) Ferlay, S.; Mallah, T.; Ouaches, R.; Veillet, P.; Verdaguer, M. *Nature* **1995**, *378*, 701.
(10) Sato, O.; Iyoda, T.; Fujishima, A.; Hashimoto, K. *Science* **1996**, *271*, 49.
(11) Sato, O.; Iyoda, T.; Fujishima, A.; Hashimoto, K. *Science* **1996**, *272*, 704.
(12) Holmes, S. M.; Girolami, G. S. *Mol. Cryst. Liq. Cryst. Sci. Technol., Sect. A* **1997**, *305*, 279.
(13) Holmes, S. M.; Girolami, G. S. *J. Am. Chem. Soc*. **1999**, *121*, 5593. Hatlevik, Ø.; Buschmann, W. E.; Zhang, J.; Manson, J. L.; Miller, J. S. *Adv. Mater*. **1999**, *11*, 914.
(14) Buschmann, W. E.; Ensling, J.; Gütlich, P.; Miller, J. S. *Chem.−Eur. J*. **1999**, *5*, 3019. Ferlay, S.; Mallah, T.; Ouahes, R.; Veillet, P.; Verdaguer, M. *Inorg. Chem*. **1999**, *38*, 229.
(15) Larionova, J.; Sanchiz, J.; Golhen, S.; Ouahab, L.; Kahn, O. *Chem. Commun*. **1998**, 953. Kahn, O.; Larionova, J.; Ouahab, L. *Chem. Commun*. **1999**, 945.
(16) Larionova, J.; Kahn, O.; Golhen, S.; Ouahab, L.; Clerac, R. *J. Am. Chem. Soc*. **1998**, *120*, 13088. Zhong, Z. J.; Seino, H.; Mizobe, Y.; Hidai, M.; Verdaguer, M.; Ohkoshi, S.; Hashimoto, K. *Inorg. Chem*. **2000**, *39*, 5095.
(17) (a) Langenberg, K. V.; Batten, S. R.; Berry, K. J.; Hockless, D. C. R.; Moubaraki, B.; Murray, K. S. *Inorg. Chem*. **1997**, *36*, 5006. (b) Parker, R. J.; Hockless, D. C.; Moubaraki, B.; Murray, K. S.; Spiccia, L. *Chem. Commun*. **1996**, 2789. (c) Zhong, Z. J.; Seino, H.; Mizobe, Y.; Hidai, M.; Fujishima, A.; Ohkoshi, S.; Hashimoto, K. *J. Am. Chem. Soc*. **2000**, *122*, 2952. (d) Larionova, J.; Gross, M.; Pilkington, M.; Audres, H.; Stoeckli-Evans, H.; Gudel, H. U.; Decurtins, S. *Angew. Chem., Int. Ed*. **2000**, *39*, 1605. (e) Sieklucka, B.; Szklarzewcz, J.; Kemp, T. J.; Errington, W. *Inorg. Chem*. **2000**, *39*, 5156. (f) Berseth, P. A.; Sokol, J. J.; Shores, M. P.; Heinrich, J. L.; Long, J. R. *J. Am. Chem. Soc*. **2000**, *122*, 9655. (g) Vostrikova, K. E.; Luneau, D.; Wernsdorfer, W.; Rey, P.; Verdaguer, M. *J. Am. Chem. Soc*. **2000**, *122*, 718. (h) Rogez, G.; Marvilliers, A.; Riviere, E.; Audiere, J.-P.; Lloret, F.; Varret, F.; Goujon, A.; Mendenez, N.; Girerd, J. J.; Mallah, T. *Angew. Chem., Int. Ed*. **2000**, *39*, 2885. (i) Marvilliers, A.; Pei, Y.; Boquera, J. C.; Vostrikova, K. E.; Paulsen, C.; Riviere, E.; Audiere, J.-P.; Mallah, T. *Chem. Commun*. **1999**, 1951. (j) Gembicky, M.; Boca, R.; Renz, F. *Inorg. Chem. Commun*. **2000**, *3*, 662.
(18) Ohba, M.; Maruone, N.; Okawa, H.; Enoki, T.; Latour, J.-M. *J. Am. Chem. Soc*. **1994**, *116*, 11566. Ohba, M.; Fukita, N.; Okawa, H. *J. Chem. Soc., Dalton Trans*. **1997**, 1733.
(19) Ohba, M.; Usuki, N.; Fukita, N.; Okawa, H. *Inorg. Chem*. **1998**, *37*, 3349. Colacio, E.; Dominguez-Vera, J. M.; Ghazi, M.; Kivekas, R.; Moreno, J. M.; Pajunen, A. *J. Chem. Soc., Dalton Trans*. **2000**, 505.
(20) (a) Kou, H.-Z.; Wang, H.-M.; Liao, D.-Z.; Cheng, P.; Jiang, Z.-H.; Yan, S.-P.; Huang, X.-Y.; Wang, G.-L. *Aust. J. Chem*. **1998**, *51*, 661. (b) Kou, H.-Z.; Liao, D.-Z.; Jiang, Z.-H.; Yan, S.-P.; Wu, Q.-J.; Gao, S.; Wang, G.-L. *Inorg. Chem. Commun*. **2000**, *3*, 151. (c) Zhan, S.-Z.; Guo, D.; Zhang, X.-Y.; Du, C.-X.; Zhu, Y.; Yang, R.-N. *Inorg. Chim. Acta* **2000**, *298*, 57. (d) Ferbinteanu, M.; Tanase, S.; Andruh, M.; Journaux, Y.; Cimpoesu, F.; Strenger, I.; Riviere, E. *Polyhedron* **1999**, *18*, 3019. (e) Shyu, H. L.; Wei, H. H.; Wang, Y. *Inorg. Chim. Acta* **1997**, *258*, 81.

10.1021/ic010282j CCC: $20.00
Published on Web 10/05/2001

magnetic properties observed. It has been noted that great emphasis has been laid on the magnetic studies of cyano-bridged nickel(II)−iron(III) assemblies based on $[NiL]^{2+}$ (L = chelating ligands) and $[Fe(CN)_6]^{3-}$ building blocks.[17a,18,19,26,30,36,38] Mallah and co-workers have recently presented a cyano-bridged Ni^{II}−Cr^{III} assembly $[Ni(cyclam)]_3[Cr(CN)_6]_2\cdot 6H_2O$ with a corrugated 2D honeycomb molecular structure.[27a] Magnetic studies show that ferromagnetic coupling operates between adjacent Ni(II) and Cr(III) metal ions and that no magnetic ordering was observed. More recently, they briefly described another Ni^{II}−Cr^{III} complex $[Ni(TMC)]_3[Cr(CN)_6]_2\cdot 12H_2O$ (TMC = 1,4,8,11-tetramethyl-1,4,8,11-tetraazacyclotetradecane) with a similar structure but with an antiferromagnetic phase transition at T_N = 14.0 K.[27b] Apparently, the factors that control the magnetic properties are not clear yet, and more such examples are needed. In this context, we characterized two cyano-bridged Ni^{II}−Cr^{III} complexes of formulas $[NiL^1]_3[Cr(CN)_6]_2\cdot 7H_2O$ (**1**) and $[NiL^2]_3[Cr(CN)_6]_2\cdot 9H_2O$ (**2**) (L^1 = 3,10-dimethyl-1,3,5,8,10,12-hexaazacycloctadecane and L^2 = 3,10-diethyl-1,3,5,8,10,12-hexaazacycloctadecane).

It has been shown that $[Cr(CN)_5(NO)]^{3-}$ is a good building block and can be used to construct new magnetic materials.[12] Whether the NO^+ group can form a linear Cr−N═O−M′ bridge remains an unanswered question. In a previous paper, we have shown that the 2D honeycomb-like assembly $[NiL^1]_3[Cr(CN)_5(NO)]_2\cdot 10H_2O$ exhibits ferromagnetic ordering at 4.5 K and the NO^+ group does not participate in bridging based on the single-crystal X-ray diffraction analysis.[34] To gain further evidence on the binding modes of $[Cr(CN)_5(NO)]^{3-}$ with transition-metal complexes, we prepared another assembly, $[NiL^2]_3[Cr(CN)_5(NO)]_2\cdot 9H_2O$ (**3**).

Also, the preparation of a novel 2D brick wall-like complex $[NiL^2]_3[Fe(CN)_6]_2\cdot 12H_2O$[30b] constructed from $[NiL^2]^{2+}$ and $[Fe(CN)_6]^{3-}$ led us to study the reactions of $[NiL^2]^{2+}$ with $[Cr(CN)_6]^{3-}$ or $[Cr(CN)_5(NO)]^{3-}$ in order to see whether the same topology could be obtained.

In this paper, we will present the synthesis, single-crystal structure analyses, and magnetic properties of the new complexes. We will also contrast the magnetic properties of the $Cr(CN)_6$ system with those of the $Cr(CN)_5(NO)$ analogue to provide a possible interpretation of the difference in magnetism for the two systems.

Results and Discussion

The IR spectra of complexes **1** and **2** show two sharp bands (2154 and 2129 cm^{-1} for **1** and 2155 and 2123 cm^{-1} for **2**) in the range 2000−2200 cm^{-1} that are attributed to C≡N stretching modes. The splitting of ν(C≡N) indicates the formation of Cr−CN−Ni linkages.

For **3**, the shift of ν(C≡N) to a higher wavenumber (2142 cm^{-1}) compared with that of $K_3[Cr(CN)_5(NO)]$ (2120 cm^{-1})[40] suggests the formation of CN^- bridges, as observed for $[NiL^1]_3[Cr(CN)_5(NO)]_2\cdot 10H_2O$.[34] Further, the blue shift (1670 cm^{-1}) of ν(N═O) with respect to that of $K_3[Cr(CN)_5(NO)]$ (1630 cm^{-1})[40] also suggests the distortion of $[Cr(CN)_5(NO)]^{3-}$ from C_{4v} symmetry as a result of the formation of Cr−C≡N−Ni linkages and that the cyanide ligand trans to the NO ligand has been involved in bridging.

The yellow complexes are insoluble in most organic and inorganic solvents and stable in air.

Description of Structures. Complexes **2** and **3** crystallize in the space group $P\bar{3}$, while complex **1** is in $C2/c$. Although the unit cell of **1** is monoclinic, the structures of the three complexes similarly consist of a neutral cyano-bridged stair-shaped layered honeycomb-like Ni_3Cr_2 network. Labeled ORTEP plots of the units for complexes **1**−**3** are shown in Figures 1, 3, and 5, respectively. Selected bond distances and angles for the complexes are listed in Tables 1−3, respectively.

$[NiL^1]_3[Cr(CN)_6]_2\cdot 7H_2O$ (1). Each $[Cr(CN)_6]^{3-}$ unit uses three *cis*-C≡N groups to connect with three $[NiL^1]^{2+}$ groups, whereas the remaining CN^- groups are monodentate. The adjacent Cr···Ni distances are 5.294(1) Å for Cr···Ni(2), 5.300(2) Å for Cr···Ni(1), and 5.259(1) Å for Cr···Ni(2A), respectively (A denotes the symmetry operation $-x + 0.5, y + 0.5, -z + 0.5$). Each $[NiL^1]$ unit is linked to two $[Cr(CN)_6]^{3-}$ ions in trans positions. Four secondary amine nitrogen atoms of the macrocycle coordinate to the nickel center in the equatorial plane, with average Ni−N distances of 2.071(3) Å for Ni(1) and 2.061(4) Å for Ni(2). Two nitrogen atoms of the bridging C≡N ligands axially coordinate to the Ni(II) ions, with

(21) Marvillers, A.; Parsons, S.; Riviere, E.; Audiere, J.-P.; Mallah, T. *Chem. Commun*. **1999**, 2217. Zou, J. Z.; Hu, X. D.; Duan, C. Y.; Xu, Z.; You, X. Z.; Mak, T. C. W. *Transition Met. Chem*. **1998**, *23*, 477. Lu, T.-B.; Xiang, H.; Li, X.-Y.; Su, C.-Y.; Mao, Z.-W.; Ji, L.-N. *Chem. J. Chin. Univ*. **2000**, *21*, 187.
(22) Colacio, E.; Dominguez-Vera, J. M.; Ghazi, M.; Kivekas, R.; Klinga, M.; Moreno, J. M. *Chem. Commun*. **1998**, 1071. Matsumoto, N.; Sunatsuki, Y.; Miyasaka, H.; Hashimoto, Y.; Luneau, D.; Tuchagues, J.-P. *Angew. Chem., Int. Ed*. **1999**, *38*, 171.
(23) Bertini, I.; Luchinat, C.; Mani, F.; Scozzafava, A. *Inorg. Chem*. **1980**, *19*, 1333.
(24) Kou, H.-Z.; Liao, D.-Z.; Cheng, P.; Jiang, Z.-H.; Yan, S.-P.; Wang, G.-L.; Yao, X.-K.; Wang, H.-G. *J. Chem. Soc., Dalton Trans*. **1997**, 1503. Fu, D. G.; Chen, J.; Tan, X. S.; Jiang, L. J.; Zhang, S. W.; Tang, W. X. *Inorg. Chem*. **1997**, *36*, 220.
(25) Zhang, H.-X.; Tong, Y.-X.; Chen, Z.-N.; Yu, K.-B.; Kang, B.-S. *J. Organomet. Chem*. **2000**, *598*, 63.
(26) Ohba, M.; Okawa, H.; Ito, T.; Ohto, A. *J. Chem. Soc., Chem. Commun*. **1995**, 1545. Ohba, M.; Okawa, H.; Fukita, N.; Hashimoto, Y. *J. Am. Chem. Soc*. **1997**, *119*, 1011. Kou, H.-Z.; Bu, W.-M.; Liao, D.-Z.; Cheng, P.; Jiang, Z.-H.; Yan, S.-P.; Fan, Y.-G.; Wang, G.-L. *J. Chem. Soc., Dalton Trans*. **1998**, 4161.
(27) (a) Ferlay, S.; Mallah, T.; Vaissermann, J.; Bartolome, F.; Veillet, P.; Verdaguer, M. *J. Chem. Soc., Chem. Commun*. **1996**, 2481. (b) Mallah, T.; Marvilliers, A.; Riviere, E. *Philos. Trans. R. Soc. London, Ser. A* **1999**, *357*, 3144.
(28) Miyasaka, H.; Ieda, H.; Matsumoto, N.; Re, N.; Crescenzi, R.; Floriani, C. *Inorg. Chem*. **1998**, *37*, 255.
(29) Miyasaka, H.; Matsumoto, N.; Okawa, H.; Re, N.; Gallo, E.; Floriani, C. *Angew. Chem., Int. Ed. Engl*. **1995**, *34*, 1446. Miyasaka, H.; Matsumoto, N.; Okawa, H.; Re, N.; Gallo, E.; Floriani, C. *J. Am. Chem. Soc*. **1996**, *118*, 981.
(30) (a) Kou, H.-Z.; Gao, S.; Bu, W.-M.; Liao, D.-Z.; Ma, B.-Q.; Jiang, Z.-H.; Yan, S.-P.; Fan, Y.-G.; Wang, G.-L. *J. Chem. Soc., Dalton Trans*. **1999**, 2477. (b) Kou, H.-Z.; Gao, S.; Ma, B.-Q.; Liao, D.-Z. *Chem. Commun*. **2000**, 1309. (c) Kou, H.-Z.; Bu, W.-M.; Gao, S.; Liao, D.-Z.; Jiang, Z.-H.; Yan, S.-P.; Fan, Y.-G.; Wang, G.-L. *J. Chem. Soc., Dalton Trans*. **2000**, 2996. (d) Colacio, E.; Dominguez-Vera, J. M.; Ghazi, M.; Kivekas, R.; Lloret, F.; Moreno, J. M.; Stoeckli-Evans, H. *Chem. Commun*. **1999**, 987.
(31) Re, N.; Gallo, E.; Floriani, C.; Miyasaka, H.; Matsumoto, N. *Inorg. Chem*. **1996**, *35*, 5964.
(32) Miyasaka, H.; Matsumoto, N.; Re, N.; Gallo, E.; Floriani, C. *Inorg. Chem*. **1997**, *36*, 670.
(33) Re, N.; Crescenzi, R.; Floriani, C.; Miyasaka, H.; Matsumoto, N. *Inorg. Chem*. **1998**, *37*, 2717.
(34) Kou, H.-Z.; Gao, S.; Ma, B.-Q.; Liao, D.-Z. *Chem. Commun*. **2000**, 713.
(35) Larionova, J.; Kahn, O.; Golhen, S.; Ouahab, L.; Clerac, R. *J. Am. Chem. Soc*. **1999**, *121*, 3349.
(36) El Fallah, M. S.; Rentschler, E.; Caneschi, A.; Sessoli, R.; Gatteschi, D. *Angew. Chem., Int. Ed. Engl*. **1996**, *35*, 1947.
(37) Ohba, M.; Usuki, N.; Fukita, N.; Okawa, H. *Angew. Chem., Int. Ed*. **1999**, *38*, 1795.
(38) Zhang, S.-W.; Fu, D.-G.; Sun, W.-Y.; Hu, Z.; Yu, K.-B.; Tang, W.-X. *Inorg. Chem*. **2000**, *39*, 1142.
(39) Sra, A. K.; Andruh, M.; Kahn, O.; Golhen, S.; Ouahab, L.; Yakhmi, J. V. *Angew. Chem., Int. Ed*. **1999**, *38*, 2606.
(40) Gans, P.; Sabatini, A.; Sacconi, L. *Inorg. Chem*. **1966**, *5*, 1877.

Table 1. Selected Bond Lengths (Å) and Angles (deg) for $[NiL^1]_3[Cr(CN)_6]_2 \cdot 7H_2O$ (**1**)[a]

Bond Length (Å)			
Cr−C(1)	2.059(5)	Cr−C(2)	2.071(4)
Cr−C(3)	2.063(5)	Cr−C(4)	2.089(4)
Cr−C(5)	2.071(4)	Cr−C(6)	2.059(5)
Ni(1)−N(4)	2.143(3)	Ni(1)−N(7)	2.074(3)
Ni(1)−N(8)	2.068(3)	Ni(2)−N(9)	2.061(4)
Ni(2)−N(10)	2.056(3)	Ni(2)−N(11)	2.048(4)
Ni(2)−N(12)	2.070(4)	Ni(2)−N(1)	2.100(4)
Ni(2)−N(5B)	2.103(4)	C(2)−N(2)	1.145(6)
C(1)−N(1)	1.148(5)	C(4)−N(4)	1.143(5)
C(3)−N(3)	1.145(6)	C(6)−N(6)	1.139(6)
C(5)−N(5)	1.139(5)		
Angle (deg)			
N(1)−C(1)−Cr	176.5(4)	N(2)−C(2)−Cr	174.3(4)
C(3)−N(3)−Cr	176.5(5)	C(4)−N(4)−Cr	172.1(3)
C(5)−N(5)−Cr	175.3(4)	C(6)−N(6)−Cr	176.9(6)
Ni(2)−N(1)−C(1)	174.2(4)	C(5)−N(5)−Ni(2A)	166.7(4)
Ni(1)−N(4)−C(4)	166.3(3)		

[a] Symmetry transformations used to generate equivalent atoms: A, $-x + {}^1/_2, y + {}^1/_2, -z + {}^1/_2$; B, $-x + {}^1/_2, y + -{}^1/_2, -z + {}^1/_2$.

Table 2. Selected Bond Lengths (Å) and Angles (deg) for $[NiL^2]_3[Cr(CN)_6]_2 \cdot 9H_2O$ (**2**)

Bond Length (Å)			
Cr−C(1)	2.072(5)	Cr−C(2)	2.081(6)
Ni−N(4)	2.055(5)	Ni−N(3)	2.084(5)
Ni−N(1)	2.094(4)	N(1)−C(1)	1.132(6)
C(2)−N(2)	1.136(7)		
Angle (deg)			
C(1)−N(1)−Ni	165.2(5)	N(1)−C(1)−Cr	175.3(5)
N(2)−C(2)−Cr	176.1(6)		

Table 3. Selected Bond Lengths (Å) and Angles (deg) for $[NiL^2]_3[Cr(CN)_5(NO)]_2 \cdot 9H_2O$ (**3**)

Bond Length (Å)			
Ni−N(4)	2.063(4)	Ni−N(3)	2.080(4)
Ni−N(2)	2.080(3)	Cr−N	1.900(5)
Cr−C(1)	1.900(5)	Cr−C(2)	2.058(4)
C(2)−N(2)	1.149(5)	C(1)−N(1)	1.208(6)
Angle (deg)			
N(2)−C(2)−Cr	176.3(3)	N(1)−C(1)−Cr	176.2(5)
C(2)−N(2)−Ni	163.3(3)	O−N−Cr	176.2(5)

Ni−N_{ax} contacts of 2.143(3) Å for Ni(1)−N(4) and 2.101(4) Å (average) for Ni(2)−N, respectively, which are slightly larger than those of the corresponding Ni−N_{eq} bonds. The bridging cyano ligands coordinate to the nickel(II) ions, with the Ni−N≡C bond angles ranging from 166.3(3)° to 174.2(4)°. The coordination symmetry about the Cr atom is a distorted octahedron, and the Cr−C≡N groups are nearly linear. The Cr−C distances range from 2.053(5) to 2.088(4) Å, which lie in the normal range. The particular local molecular disposition leads to a honeycomb-like layered structure (Figure 2a), similar to that reported for the 2D honeycomb-like PB analogues.[27,30] The projection along the *a* axis (Figure 2b) shows the stacking of the stair-shaped layers. The layers align along the *c* axis with a separation of ca. 9.7 Å, and the shortest interlayer metal−metal distance is 6.953 Å for Ni···Cr. The water molecules are positioned between the layers and linked to the terminal CN ligands of $[Cr(CN)_6]^{3-}$, the nitrogen atom of the macrocyclic ligand L^1, and the other water molecules via hydrogen bonding. Adjacent layers are connected through hydrogen bonds, yielding a quasi-3D network.

$[NiL^2]_3[Cr(CN)_6]_2 \cdot 9H_2O$ (2). The structure of complex **2** consists of a neutral cyano-bridged stair-shaped layer network with the stoichiometry of $[NiL^2]_3[Cr(CN)_6]_2$. Each $[NiL^2]$ unit is linked to two $[Cr(CN)_6]^{3-}$ ions in trans positions. Each

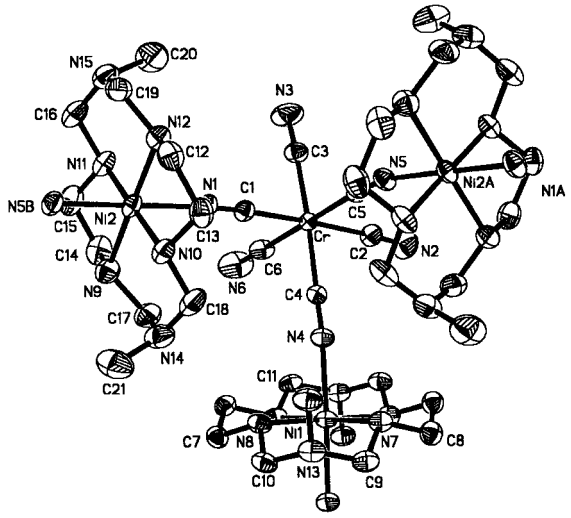

Figure 1. ORTEP plot of **1**.

$[Cr(CN)_6]^{3-}$ unit uses three C_3 rotational symmetry related cis C≡N^- groups to connect with three $[NiL^2]^{2+}$, whereas the three remaining symmetry related cis CN^- groups are nonbridging. The nickel(II) ion is nearly octahedral, with the Ni−N bond distances ranging from 2.055(5) to 2.084(5) Å, and the cyanide nitrogen atoms are sited at the axial positions (Ni−N_{cyano} = 2.094(4) Å). The average Cr−C and C≡N distances are 2.076(6) and 1.134(7) Å, and the Cr−C≡N groups do not deviate significantly from linearity (175.3(5)° and 176.1(6)°). The Ni−N≡C bond angle is 165.2(5)°. The adjacent Cr···Ni distance is 5.246(1) Å.

The local molecular disposition leads to a honeycomb-like structure (Figure 4a). The 2D layer is not planar but adopts a chair conformation (Figure 4b), which is similar to that of the analogous complexes.[27,30] The layers align along the *c* axis with a separation of ca. 9.53 Å, and the nearest interlayer metal−metal distance is 7.822 Å for Ni···Cr. The water molecules are positioned between the layers and linked to the terminal CN ligands of $[Cr(CN)_6]^{3-}$, the nitrogen atom of the macrocyclic ligand L^2, and the other water molecules via hydrogen bonding.

$[NiL^2]_3[Cr(CN)_5(NO)]_2 \cdot 9H_2O$ (3). Complex **3** is isomorphous with **2**. Each $[Cr(CN)_5(NO)]^{3-}$ unit uses three *cis*-C≡N groups to connect with three $[NiL^2]^{2+}$ groups, whereas the two remaining CN^- and the NO^+ groups are monodentate. The presence of a C_3 rotational axis at Cr(I) results in the disorder of NO by about three coordination positions. Therefore, the corresponding Cr−N and Cr−C bond lengths are statistically averaged to be 1.900(5) Å, in good agreement with the averaged value (1.925 Å) in the ordered structure $[Co(en)_3][Cr(CN)_5(NO)] \cdot 2H_2O$[41] (Cr−C = 2.033 Å and Cr−N = 1.708 Å). The adjacent Cr···Ni distance is 5.226(1) Å. Two nitrogen atoms of the bridging C≡N ligands axially coordinate to the Ni(II) ions with the Ni−N_{ax} contacts of 2.080(3) Å, which are slightly larger than those of the corresponding Ni−N_{eq} bonds (average value = 2.071(4) Å). The bridging cyanide ligands coordinate to the nickel(II) ions in a bent fashion, with the Ni−N≡C bond angle of 163.3(3)°. The particular local molecular disposition leads to a honeycomb-like layered structure, which is similar to that of **2**. The shortest interlayer metal−metal distance is 7.647 Å for Cr···Ni, while the interlayer separation is 9.31 Å.

Magnetic Properties. The temperature dependence of the magnetic susceptibilities for **1**−**3** was measured in a field of

(41) Enemark, J. H.; Quinby, M. S.; Reed, L. L.; Steuck, M. J.; Walthers, K. K. *Inorg. Chem.* **1970**, *9*, 2397.

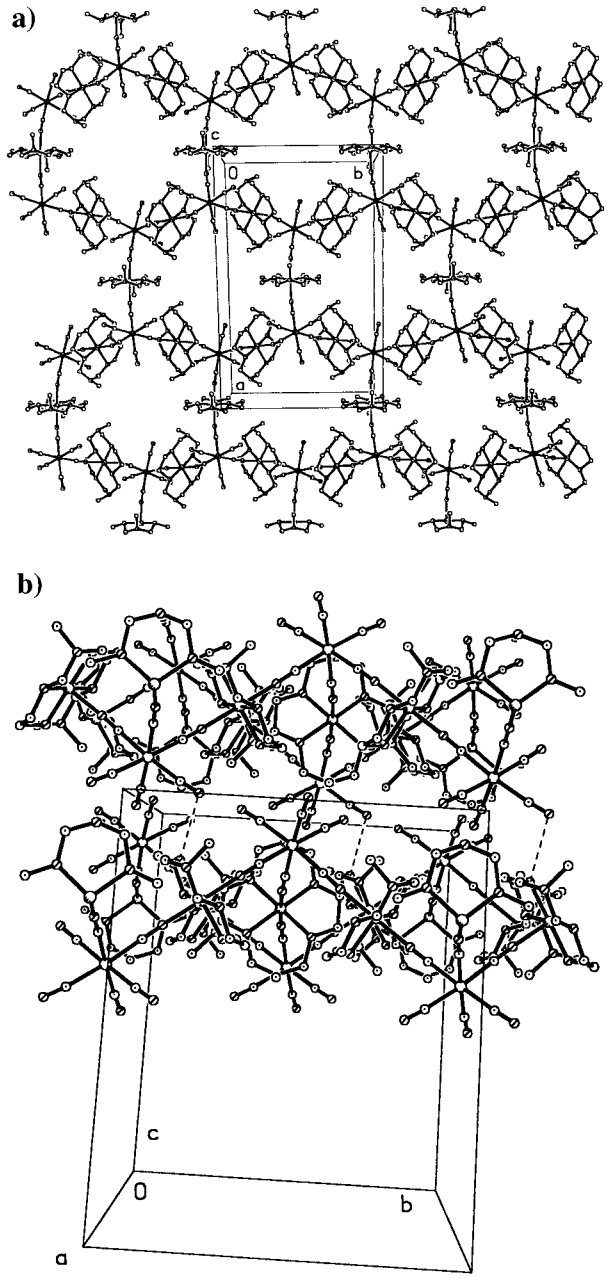

Figure 2. (a) Projection showing the 2D layer of Cr_6Ni_6 hexagons for **1**. (b) Stacking of the stair-shaped layers for **1**.

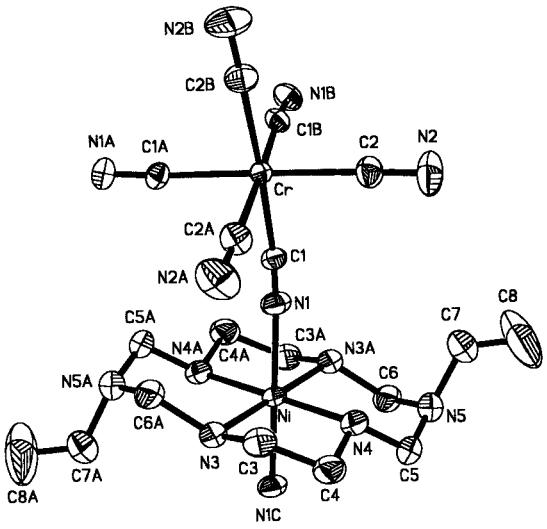

Figure 3. ORTEP plot of **2**.

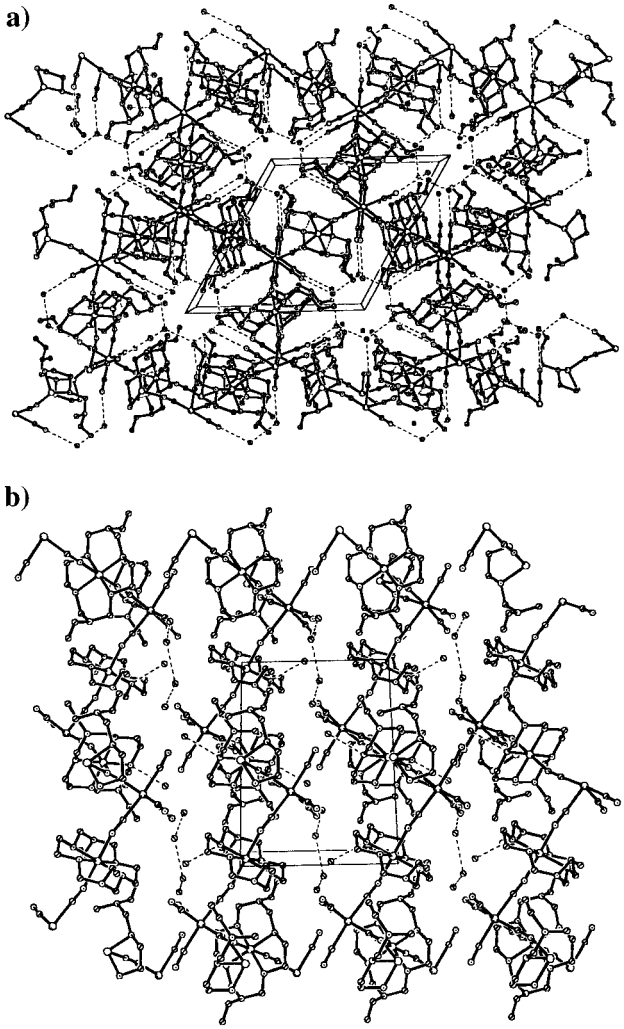

Figure 4. (a) Projection showing the 2D layer containing Cr_6Ni_6 hexagons for **2**. (b) Stacking of the stair-shaped layers for **2**.

10 kOe, and the field-cooled magnetization (FCM) was measured at low temperatures to confirm the magnetic ordering.

Complex 1. A plot of $\chi_m T$ versus T is shown in Figure 6, where χ_m is the magnetic susceptibility per Ni_3Cr_2 unit. With the decrease of the temperature, $\chi_m T$ increases slowly down to ca. 30 K and then sharply, reaching a maximum value of 57.6 emu K mol^{-1} (21.5 μ_B) at 14.3 K. The $\chi_m T$ value (7.7 emu K mol^{-1}, 7.8 μ_B) at room temperature is slightly higher than expected (6.75 emu K mol^{-1}, 7.3 μ_B) for the spin-diluted Ni_3Cr_2 system. The maximum value 57.6 emu K mol^{-1} (21.5 μ_B) is much larger than the value of 21.0 emu K mol^{-1} (13.0 μ_B) for the $S_T = 6$ state resulting from the ferromagnetic coupling of three nickel(II) ions ($S = 1$) and two chromimum(III) ions ($S = {}^3/_2$), strongly suggestive of the occurrence of magnetic ordering (i.e., a magnetic phase transition). Below 14.3 K, $\chi_m T$ decreases rapidly, which may be due to the interlayer antiferromagnetic interaction, the field saturation of the magnetization, and the zero-field splitting effect of the nickel(II) ions in axially elongated octahedral surroundings.

The FCM versus T plot (Figure 6, inset) shows a sharp peak at 12.6 K, suggesting an antiferromagnetic order below ca. 12.6 K. This indicates that an interlayer antiferromagnetic interaction operates principally.

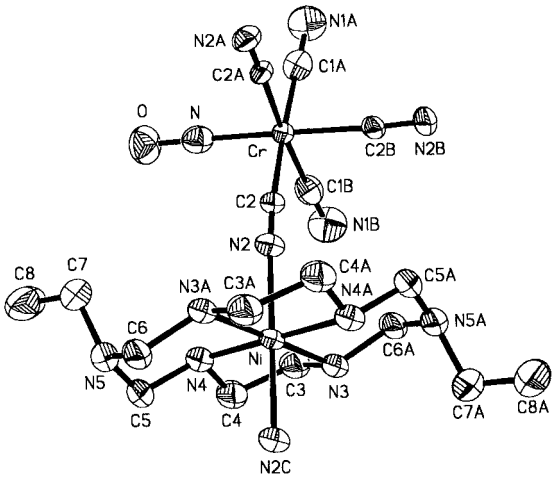

Figure 5. ORTEP plot of **3**.

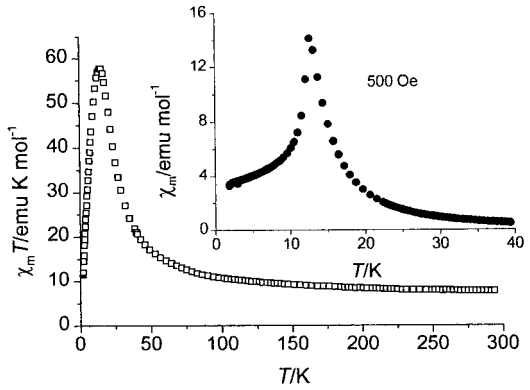

Figure 6. Temperature dependence of $\chi_m T$ for **1** (inset: FCM curve of **1**).

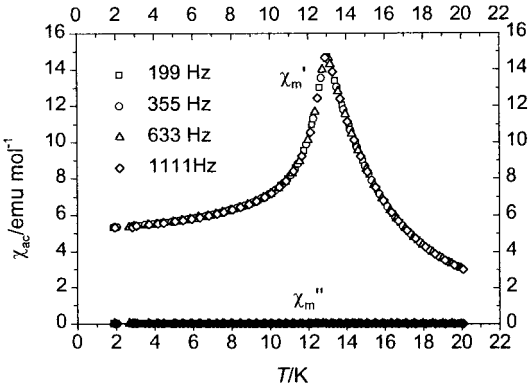

Figure 7. Real (χ) and imaginary (χ'') ac magnetic susceptibilities as a function of temperature taken at 199, 355, 633, and 1111 Hz for **1**.

The temperature dependence of ac magnetic susceptibilities presented in Figure 7 shows that the real part of the zero-field ac magnetic susceptibility (χ') has a maximum at ca. 13.0 K for frequencies of 199, 355, 633, and 1111 Hz and that the out-of-phase component of ac magnetic susceptibility (χ'') is negligibly small, indicating antiferromagnetic ordering below 13.0 K.

The field dependence of the magnetization at 1.8 K reveals a hysteresis loop with a coercive field of 70 Oe and a remnant magnetization of about 0.11 Nβ (Figure 8). The magnetization shows a pronounced sigmoidal behavior, which suggests the metamagnetic nature of **1**. The magnetization first increases slowly with the increased field and then sharply, showing a transition from an antiferromagnetic arrangement to a ferromagnetic arrangement between the layers. The critical field (the lowest field which is used to reverse the interlayer antiferromagnetic interaction) is ca. 1.6 kOe at 1.8 K. The *M* versus *H* curve at 1.8 K shows a rapid saturation above 1.6 kOe, reaching a value of 11.3 Nβ at 60 kOe, which confirms ferromagnetic coupling between the Cr(III) and Ni(II) ions through cyano bridges.

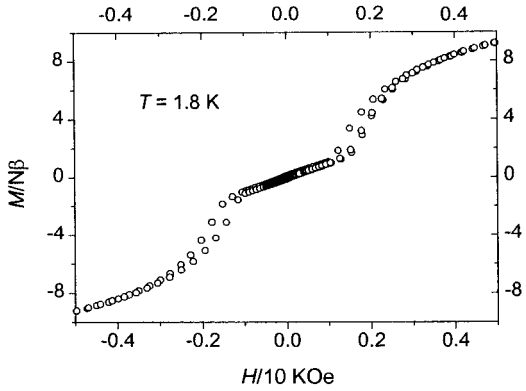

Figure 8. Magnetic hysteresis loop at 1.8 K for **1**.

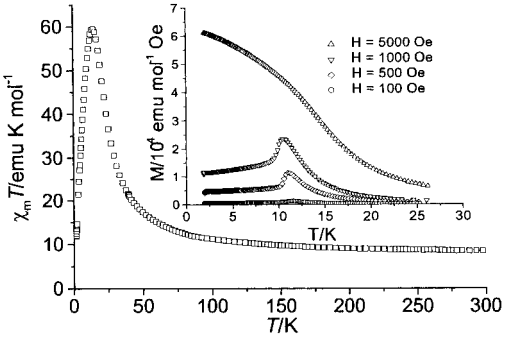

Figure 9. Temperature dependence of $\chi_m T$ for **2** in an applied field of 10 kOe (inset: FCM curve of **2**).

Complex 2. The plot of $\chi_m T$ versus *T* for **2** shown in Figure 9 ($H = 10$ kOe) is similar to that for **1**. The $\chi_m T$ value (8.3 emu K mol^{-1}, 8.1 μ_B) at 300 K is higher than expected (6.75 emu K mol^{-1}, 7.3 μ_B) for dilute three nickel(II) ions ($S = 1$) and two chromium(III) ions ($S = {}^3/_2$). With the decrease of the temperature, $\chi_m T$ increases smoothly down to ca. 40 K and then sharply, reaching a maximum value of 59.4 emu K mol^{-1} (21.8 μ_B) at 14.6 K. Below 14.6 K, $\chi_m T$ decreases rapidly, which is due to the combination of magnetic field saturation and the zero-field splitting effect of the nickel(II) ions. The gradual increase in $\chi_m T$ from 300 to 40 K proves the presence of ferromagnetic coupling within the Ni_3Cr_2 sheet of **2**.

The field-cooled magnetizations measured at 100, 500, and 1000 Oe, respectively, show a peak of χ_m at 11.4 K, suggesting an antiferromagnetic ordering (see inset of Figure 9). The FCM curve in 5000 Oe exhibits no maximum, indicating the metamagnetic properties of **2**. The onset of an antiferromagnetic phase transition is further confirmed by the temperature dependence of ac molar magnetic susceptibility, displayed in Figure 10. The real part of the zero-field ac magnetic susceptibilities (χ_{ac}') possesses a maximum at ca. 11.9 K. The absence of χ_{ac}'' suggests that T_N of complex **2** is about 11.9 K.[42]

The *M* versus *H* curve at 1.8 K (Figure 11) shows a rapid saturation above 1.5 kOe, reaching a value of 11.6 Nβ at 50

(42) Bohm, A.; Vazquez, C.; McLean, R. S.; Calabrese, J. C.; Kalm, S. E.; Manson, J. L.; Epstein, A. J.; Miller, J. S. *Inorg. Chem.* **1996**, *35*, 3083.

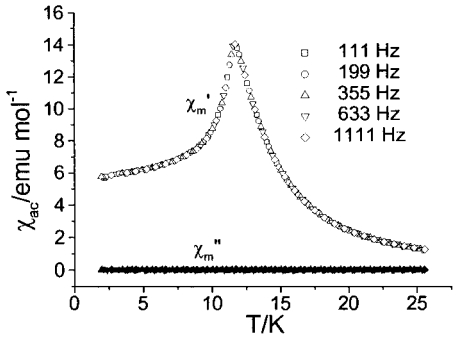

Figure 10. Real (χ) and imaginary (χ'') ac magnetic susceptibilities as a function of temperature taken at 111, 199, 355, 633, and 1111 Hz for **2**.

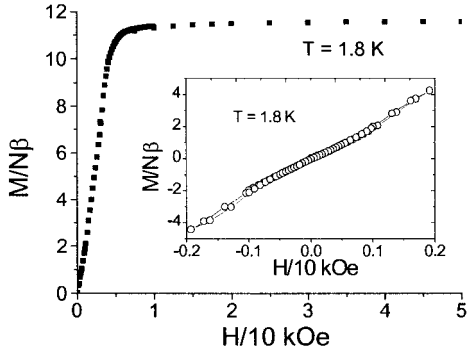

Figure 11. Field dependence of magnetization for **2** at 1.8 K (inset: magnetic hysteresis loop at 1.8 K for **2**).

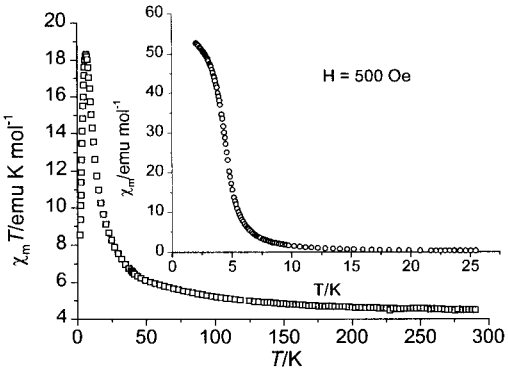

Figure 12. Temperature dependence of $\chi_m T$ for **3** in an applied field of 10 kOe (inset: FCM for **3**).

kOe, which confirms ferromagnetic coupling between the Cr(III) and Ni(II) ions through cyano bridges. The field dependence of the magnetization at 1.8 K reveals no hysteretic behavior (see inset of Figure 11). The magnetization shows a sigmoidal behavior, which suggests the metamagnetic nature of **2**. The critical field is ca. 1.5 kOe at 1.8 K.

Complex 3. A plot of $\chi_m T$ versus T for **3** is shown in Figure 12, where χ_m is the magnetic susceptibility per Ni_3Cr_2 unit. The $\chi_m T$ value at 290 K is ca. 4.5 emu K mol^{-1} (6.0 μ_B), which increases smoothly and then sharply with the decrease of the temperature, reaching a maximum value of 18.3 emu K mol^{-1} (11.3 μ_B) at 6.6 K, strongly suggestive of the occurrence of magnetic ordering. Below 6.6 K, $\chi_m T$ decreases rapidly, which may be due to field saturation of the magnetization and the zero-field splitting effect of the nickel(II) ions.

The FCM curve (see inset of Figure 12) suggests the ferromagnetic nature of **3**. The absence of a peak down to 2.0 K in the FCM curve shows the existence of an interlayer ferromagnetic interaction. The derivative curve (dFCM/dT) presents an

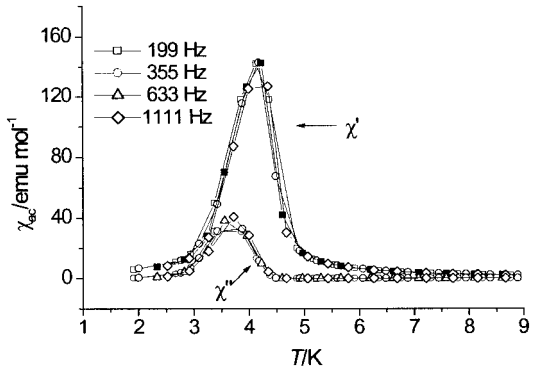

Figure 13. Real (χ) and imaginary (χ'') ac magnetic susceptibilities as a function of temperature taken at 199, 355, 633, and 1111 Hz for **3**.

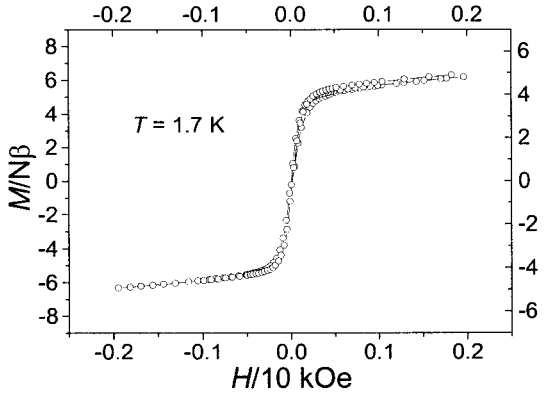

Figure 14. Magnetic hysteresis loop at 1.7 K for **3**.

extremum at 4.5 K, corresponding to the transition temperature (T_c).

The real part of the ac magnetic susceptibility (χ_{ac}') has a maximum at ca. 4.3 K accompanied by the occurrence of nonzero χ_{ac}'', suggesting that T_c of complex **3** is about 4.3 K (Figure 13). This value is much closer to that of $[NiL^1]_3[Cr(CN)_5(NO)]_2 \cdot 10H_2O$ (4.5 K).[34]

The field dependence of the magnetization (0−50 kOe) measured at 1.8 K shows rapid saturation of magnetization reaching a value of 8.0 Nβ at 50 kOe, equal to the expected $S = 4$ value of 8 Nβ for the ferromagnetic Ni_3Cr_2 system. The hysteresis loop at 1.7 K is shown in Figure 14 and displays a small coercive field of less than 10 Oe and a remnant magnetization of about 0.4 Nβ per Ni_3Cr_2 unit, typical of a soft ferromagnet.

It has been known that, as far as a 2D layered system is concerned, the combination of the intralayer ferromagnetic and the interlayer antiferromagnetic interactions is responsible for the occurrence of metamagnetic behavior. According to Ohba et al., for the cyano-bridged 2D square-like $[Ni(diamine)_2]_2[Fe(CN)_6]X$ assemblies, metamagnetic behavior occurs when the interlayer separation is less than 10 Å.[26] We have reported two cyano-bridged 2D honeycomb-like Ni_3Fe_2 complexes, which also show metamagnetic behavior.[30a,c] The structural analyses show that the interlayer separations in these complexes are ca. 9.3 Å. For **1**, the crystal packing shows that the shortest interlayer Ni(II)···Cr(III) ions (6.95 Å) are connected through the −NH···N≡C− hydrogen bond, favoring a strong interlayer antiferromagnetic interaction. It seems surprising that complex **2** exhibits a metamagnetic behavior while isomorphous complex **3** has a ferromagnetic order. This suggests that the nature of the interlayer magnetic interaction relates to the interacting metal ions Ni(II)−Cr(III) in **2** and Ni(II)−Cr(I) in **3**.

Table 4. Crystal Data and Structure Refinement for Complexes **1**−**3**

	1	**2**	**3**
formula	$C_{42}H_{90}Cr_2N_{30}Ni_3O_7$	$C_{48}H_{114}Cr_2N_{30}Ni_3O_9$	$C_{46}H_{108}Cr_2N_{30}Ni_3O_{11}$
M_R	1409.59	1529.77	1537.75
λ (Å)	0.710 73	0.710 73	0.710 73
cryst syst	monoclinic	trigonal	trigonal
space group	*C*2/*c*	$P\bar{3}$	$P\bar{3}$
a (Å)	25.929(5)	14.919(2)	14.863(2)
b (Å)	15.442(3)	14.919(2)	14.863(2)
c (Å)	19.553(4)	9.5246(19)	9.3134(19)
α (deg)	90	90	90
β (deg)	106.21(3)	90	90
γ (deg)	90	120	120
V (Å^3)	7518(3)	1835.9(5)	1781.7(5)
Z	4	1	1
cryst size (mm)	0.12 × 0.24 × 0.30	0.14 × 0.20 × 0.26	0.18 × 0.25 × 0.28
ρ_{calcd}	1.245	1.384	1.433
μ(Mo Kα) (mm^{-1})	1.076	1.110	1.146
F(000)	2968	810	814
θ_{max}	27.96	27.87	27.89
reflns collected	49 556	20 390	38 162
independent reflns	8940	2893	2802
data/restraints/params	5801/0/384	2225/0/142	2044/0/142
final *R* indices [$I > 2\sigma(I)$]	R1 = 0.0613, wR2 = 0.1642	R1 = 0.0721, wR2 = 0.1749	R1 = 0.0630, wR2 = 0.1572
R indices (all data)	R1 = 0.1051, wR2 = 0.1912	R1 = 0.0937, wR2 = 0.1878	R1 = 0.0917, wR2 = 0.1693
largest diff peak/hole (e Å^{-3})	0.817/−0.348	0.730/−0.629	0.374/−0.470

Complexes **1** and **2** possess similar magnetic behaviors. The slight difference in the long-range magnetic transition temperatures (T_N) is due to the difference in the magnitude of an interlayer antiferromagnetic interaction.[30a,c] It is known that the stronger interlayer antiferromagnetic interaction in an antiferromagnet would result in a higher T_N value. Therefore, it can be concluded that the interlayer antiferromagnetic interaction in **2** is to some extent weaker than that in **1**. The difference in the critical field (H_c) between the two complexes, 1600 Oe for **1** and 1500 Oe for **2**, also adds support to this supposition.

The small coercivity in the present complexes is probably due to the absence of irreversible movements of the domain walls.

Complexes **1** and **2** have a T_N value similar to that of the Ni_3Cr_2 analogue $[Ni(TMC)]_3[Cr(CN)_6]_2\cdot 12H_2O$.[27b] That the complex $[Ni(cyclam)]_3[Cr(CN)_6]_2\cdot 6H_2O$ does not undergo spontaneous magnetic ordering down to 2 K is probably the result of the change in the interlayer magnetic interaction with the partial loss of lattice water molecules. This could be proven by the fact that the complete dehydration of a 1D chain complex $[Cu(dien)]_3[Fe(CN)_6]_2\cdot 6H_2O$ results in a dramatic modification of the magnetic behavior, changing from ferromagnetic to overall antiferromagnetic.[20d]

The ferromagnetic interaction between the chromium(III) and nickel(II) ions can be explained by the strict orthogonality of the magnetic orbitals of Cr^{III} ($^3t_{2g}$) and Ni^{II} (^2e_g).[43] The ferromagnetic interaction between the low-spin chromium(I) and nickel(II) ions is due to the strict orthogonality of the magnetic orbitals of the Cr(I) [d^5, $(3d_{xy})^1$][44] and Ni(II) [d^8, $(d_{x^2-y^2})^1(d_{z^2})^1$] ions.[34]

Conclusions

We have synthesized and structurally characterized three new cyano-bridged 2D bimetallic magnets constructed from $[NiL^1]^{2+}$ and $[NiL^2]^{2+}$ and $[Cr(CN)_6]^{3-}$ or $[Cr(CN)_5(NO)]^{3-}$. The complexes have a stair-shaped honeycomb-like layered structure extended by Cr−C≡N−Ni linkages, and the NO^+ groups in the $[Cr(CN)_5(NO)]$ derivative do not participate in bridging. The $Cr(CN)_6$ species exhibit long-range antiferromagnetic ordering at 13.0 and 11.9 K, respectively. Metamagnetic behavior was observed in **1** and **2** below T_N, which is due to the antiferromagnetic interaction between the shortest interlayer metal··· metal ions. The $Cr(CN)_5(NO)$ complex exhibits a ferromagnetic phase transition at 4.3 K, similar to that of the reported analogue $[NiL^1]_3[Cr(CN)_5(NO)]_2\cdot 10H_2O$. The hysteresis loops show that the three complexes are soft magnets with a coercive field of 70 Oe for **1** and 11 Oe for **3**, while **2** has a hardly noticeable coercive field.

Experimental Section

Elemental analyses of carbon, hydrogen, and nitrogen were carried out with a Elementar Vario EL. The infrared spectroscopy on KBr pellets was performed on a Magna-IR 750 spectrophotometer in the 4000−400 cm^{-1} region. Variable-temperature magnetic susceptibility in the fields of 0.1, 0.5, 1, 5, and 10 kOe (FCM), zero-field ac magnetic susceptibility measurements, and field dependence magnetization were performed on a Maglab System 2000 magnetometer. Effective magnetic moments were calculated by the equation $\mu_{eff} = 2.828(\chi_m T)^{1/2}$, where χ_m is the molar magnetic susceptibility. The experimental susceptibilities were corrected for the diamagnetism of the constituent atoms (Pascal's tables).

Syntheses. The precursors $[NiL^1](ClO_4)_2$,[45] $[NiL^2](ClO_4)_2$,[45] $K_3[Cr(CN)_6]$,[46] and $K_3[Cr(CN)_5(NO)]\ H_2O$[47] were prepared by the literature methods. **Caution!** Perchlorate salts of metal complexes with organic ligands are potentially explosive and should be handled in small quantities with care.

$[NiL^1]_3[Cr(CN)_6]_2\cdot 6H_2O$ (1). To an aqueous solution (15 mL) of $[NiL^1](ClO_4)_2$ (0.3 mmol) was added dropwise, with stirring, a solution of $K_3[Cr(CN)_6]\cdot H_2O$ (0.2 mmol) in 10 mL of water. This led to the immediate precipitation of yellow microcrystals that were collected by suction filtration, washed with water, and dried in air. Anal. Calcd for $C_{42}H_{92}N_{30}O_7Cr_2Ni_3$ (1409.59): C, 35.79; N, 29.81; H, 6.58. Found: C, 35.72; N, 30.30; H, 6.72. IR (cm^{-1}, KBr): $\nu_{C\equiv N}$ 2154, 2129.

Well-shaped yellow crystals suitable for X-ray structure analysis were grown at room temperature by the slow diffusion of an orange MeCN solution (30 mL) of $[NiL^1](ClO_4)_2$ (0.15 mmol) and a yellow aqueous solution (30 mL) of $K_3[Cr(CN)_6]$ (0.15 mmol) in an H tube.

(43) Kahn, O. *Molecular Magnetism*; VCH: New York, 1993; p 251.
(44) Manoharan, P. T.; Gray, H. B. *J. Am. Chem. Soc*. **1965**, *87*, 3340.
(45) Suh, M. P.; Kang, S.-G. *Inorg. Chem*. **1988**, *27*, 2544.
(46) Bigelow, J. H.; Bailar, J. C. *Inorg. Synth*. **1946**, *2*, 203.
(47) Griffith, W. P.; Lewis, J.; Wilkinson, G. *J. Chem. Soc*. **1959**, 872.

$[NiL^2]_3[Cr(CN)_6]_2\cdot 9H_2O$ (2). Complex **2** was prepared as yellow microcrystals in a way similar to that of complex **1** except for the employment of $[NiL^2](ClO_4)_2$ replacing $[NiL^1](ClO_4)_2$. Anal. Calcd for $C_{42}H_{108}N_{30}O_9Cr_2Ni_3$ (1529.77): C, 37.69; N, 27.47; H, 7.12. Found: C, 37.67; N, 27.24; H, 7.11. IR (cm^{-1}, KBr): $\nu_{C\equiv N}$ 2155, 2123.

$[NiL^2]_3[Cr(CN)_5(NO)]_2\cdot 9H_2O$ (3). Complex **3** was prepared in a way similar to that of complex $[NiL^1]_3[Cr(CN)_5(NO)]_2\cdot 10H_2O$[34] except for the employment of $[NiL^2](ClO_4)_2$ replacing $[NiL^1](ClO_4)_2$. Anal. Calcd for $C_{46}H_{108}N_{30}O_{11}Cr_2Ni_3$ (1537.75): C, 35.93; N, 27.33; H, 7.08. Found: C, 35.79; N, 27.67; H, 7.06. IR (cm^{-1}, KBr): $\nu_{C\equiv N}$ 2142, 2111, $\nu_{O=N}$ 1670. Well-shaped yellow crystals were prepared by a slow diffuse method and subject to magnetic measurements and X-ray diffraction structural analysis.

Crystallographic Data Collection and Structure Determination. The data collections of **1**−**3** were made on a Nonius κ-CCD diffractometer using graphite-monochromated Mo Kα radiation ($\lambda = 0.710\,69$ Å) at 293 K. The structures were solved by the direct method and refined by full-matrix least-squares (SHELEXL-93) on F^2. Anisotropic thermal parameters were used for the non-hydrogen atoms and isotropic parameters for the hydrogen atoms. Hydrogen atoms were added geometrically and refined using a riding model. The pendent ethyl carbon atoms of the macrocyclic ligand L^2 in **3** experienced disorder over two positions, and a split-atom model with a 1:1 occupancy was applied. Weighted R factors (wR) and all of the goodness-of-fit (S) values are based on F^2; conventional R factors (R) are based on F, with F set to zero for negative F^2. The weighting scheme is $w = 1/[s^2F_o^2 + (0.0433P)^2 + 0.0000P]$, where $P = (F_o^2 + 2F_c^2)/3$. The crystal data are summarized in Table 4.

Acknowledgment. This work was supported by the State Key Project of Fundamental Research (Grant G1998061305), the National Natural Science Foundation of China (Grants 20023005 and 29831010), the Postdoctoral Science Foundation of China, and the Excellent Young Teachers Fund of MOE, P. R. China.

Supporting Information Available: X-ray crystallographic file in CIF format is available via the Internet. Field dependence of magnetization for **1** and **3** at 1.8 K. This material is available free of charge via the Internet at http://pubs.acs.org.

IC010282J